CONF-950808--1

Microstructural Development in PWA–1480 Electron Beam Welds - An Atom Probe Field Ion Microscopy Study.

S. S. Babu,† S. A. David and M. K. Miller

Metals and Ceramics Division, Oak Ridge National Laboratory,

Oak Ridge, TN 37831-6096.

†On assignment from The Pennsylvania State University, PA 16802.

Paper to be presented at 42nd International Field Emission Symposium, to be held at Madison, Wisconsin, USA, during August 7-11, 1995.

Please send the proofs to:

Dr. S. S. Babu

Research Scholar, Metals and Ceramics Division

Oak Ridge National Laboratory, Oak Ridge, TN 37831-6096.

Tel: (615) - 574 - 4806

Fax: (615) - 574 - 7721

Email: babuss@ornl.gov

Microstructural Development in PWA–1480 Electron Beam Welds - An Atom Probe Field Ion Microscopy Study.

S. S. Babu,† S. A. David and M. K. Miller

Metals and Ceramics Division, Oak Ridge National Laboratory, Oak Ridge, TN 37831-6096.

†On assignment from The Pennsylvania State University, PA 16802.

ABSTRACT

The microstructure development in PWA–1480 superalloy electron beam weld (Ni–11.0 at. % Al–11.5% Cr–1.9% Ti–5.1% Co–4.0 % Ta–1.3% W) was characterized. Optical microscopy revealed a branched dendritic structure in the weld metal. Transmission electron microscopy of these welds, in the as-welded condition, showed fine cuboidal (0.05 – 0.5 μm) $L1_2$-ordered γ' precipitates within the γ grains. The average volume percentage of γ' precipitates was found to be ~75%. Atom probe analyses revealed that the composition of γ matrix was Ni–4.6 at. % Al–25.5% Cr–0.4% Ti–9.4% Co–0.8% Ta–2.9% W and that of γ' precipitates was Ni–17.3 at. % Al–2.6% Cr–2.4% Ti–3.0% Co–7.4% Ta–1.3% W. These compositions were compared with the previous APFIM analyses of commercial PWA–1480 single crystals that had received conventional heat treatments. Small differences were found in the chromium and aluminum levels and these may be due to the nonequilibrium nature of phase transformations that occur during weld cooling. No solute segregation was detected at the γ–γ' interface. The APFIM results were also compared with the thermodynamic calculations of alloying element partitioning between γ and γ' using the ThermoCalc™ software.

1. Introduction

Previous weldability studies have shown that Ni_3Al type alloys can be welded successfully [1–4]. Recently, a comprehensive research program has been initiated to extend the weldability studies to single crystal Ni–base superalloys for turbine applications. It is known that the microstructure development during welding will govern the properties and reliability of these welds. Since a typical fusion welding process involves rapid heating and cooling conditions, microstructural development in these welds is expected to be complicated. During weld cooling, as the solidification proceeds through the weld, segregation of some alloying elements between dendrites is expected. Besides this segregation due to solidification, it is speculated that there may be nonequilibrium partitioning and interfacial segregation of alloying elements (such as tungsten and tantalum) between γ (fcc structure) and $\gamma'(L1_2$ ordered structure).

In this paper, the microstructure of an electron beam welded PWA–1480 single crystal superalloy was investigated. Although much information exists [5-8] on microstructure and partitioning characteristics between γ and γ' in PWA-1480 single crystals after standard heat treatments, microstructural information in welds is not available. This information is crucial in designing better welding procedures and post weld heat treatment schedules. The paper describes an atom probe field ion microscopy (APFIM) investigation to measure nonequilibrium partitioning between γ and γ' and to validate the speculation of any interfacial segregation. In addition, the measured APFIM measurements were compared with the previously published data in the PWA–1480 material after standard heat treatment [5–8]. Also, preliminary thermodynamic calculations with the use of the ThermoCalc™ program [9], to predict the microstructure development in PWA-1480 alloys, are described.

2. Experimental

2.1 Material and Welding Procedure:

Cast single crystals of PWA-1480 superalloy of composition given in Table 1 were studied. These single crystals were received after a standard heat treatment [5]. Autogeneous electron beam welds

were made on 2–3 mm thick sheets machined from single crystal bars. Full penetration welds were obtained with the following welding parameters: 100–125 kV, 7.5–10 mA, and welding speed 4.2×10^{-3} m s^{-1}. The welds were examined in the as-welded condition.

2.2. Microstructural Analysis:

Optical microscopy of the welds was performed after mechanical polishing and etching in Marbles' reagent. The samples were examined in a Philips-CM12 transmission electron microscope with EDX capability. The ORNL atom probe field ion microscope [10] was used to characterize the partitioning and the possible segregation of alloying elements at γ–γ' interfaces. The samples were imaged at 50-60K with neon and the atom probe analyses were performed with a residual neon gas pressure of 3×10^{-7} Pa and with a pulse fraction of 20%.

3. Results and Discussion

3.1 Weld Microstructural Development:

Optical microscopy of PWA-1480 welds indicated a dendritic mode of weld solidification (Fig. 1). The average dendrite arm spacing was ~30–40 μm. The weld zone was partly polycrystalline and illustrated the difficulty of maintaining the single crystalline nature in the weld zone. A low magnification transmission electron micrograph (Fig. 2a) shows a boundary between two dendrite arms. Along the interdendritic regions blocky γ' grains interlaced by thin films of γ were observed. The morphology of these blocky γ' grains with penetrated γ phase suggests that this blocky γ' formed during the final stages of solidification through a eutectic reaction, $L \rightarrow \gamma + \gamma'$. Qualitative EDX analysis indicated that the inter–dendritic regions were Cr-rich γ phase. Within the core of the dendrite, fine cuboidal $L1_2$ ordered γ' precipitates were observed (Fig. 2b). Electron diffraction confirmed the presence of γ' precipitates within the γ matrix. The size of these cuboidal γ' varied from 0.05 to 0.5 μm and the average volume fraction of γ' was found to be ~ 75%. However, the volume fraction of γ' varied from region to region (60–85 %) within a single dendrite.

The above microstructure development can be explained with the help of a quasi-binary diagram of Ni-Al-Cr alloy system, as shown in Fig. 3. With this phase diagram, one can follow various phase transformations that occur during cooling from the liquid state. To illustrate the microstructure development in the PWA-1480 alloy, the reactions in the Ni–11.0 at.% Al–11.5 at.% Cr alloy, as it solidifies from the liquid state, are discussed below. According to the equilibrium phase diagram, the solidification to γ starts at ~1698 K and is completed at ~1685 K. Since the weld cooling conditions are far from equilibrium conditions, this may not be an actual representation of the weld solidification. Therefore one has to apply Scheil [11] analysis to model weld solidification. Scheil's analysis assumes local equilibrium at the liquid–γ interface. In this case, the solidus temperature will be lowered as a result of alloying element partitioning into liquid. The liquid composition will follow the boundary between the liquid and (L+γ) phase fields as dictated by the tie lines, which are not shown in Fig. 3.

The variations of the compositions in the γ and liquid phases during such a solidification in a Ni–11.0 at.% Al–11.5 at.% Cr alloy (assuming Scheil's model) were calculated using ThermoCalc™ software [9]. These calculations assume that there is no back diffusion in the γ phase. The results are shown in Fig. 4. The calculations show that the aluminum concentration at the core of the γ dendrite (which forms at high temperature) is lower than that of the γ dendrite boundaries (which form at a lower temperature). The calculations indicate that the solidus temperature is lowered to 1635 K. ThermoCalc™ calculations also suggested that the final liquid, due to the solute enrichment, will undergo an eutectic reaction at ~1630 K as shown in Fig. 3. The eutectic γ' in the interdendritic regions is also observed in MAR-M 200 superalloys produced by directional solidification [12]. The observation, Fig. 2b, of blocky γ' interlaced with films of γ supports this mode of solidification for the weld.

Although thermodynamic calculations of Ni-Al-Cr system can be used in understanding the microstructure development during weld solidification of a superalloy, care must be taken in extending these calculations to PWA–1480 welds. The temperatures of solidification, eutectic temperature, eutectic composition, as well as the γ composition shown in Fig. 3 and 4 will be

different for PWA-1480 weld. This is due to the influence of other alloying elements including titanium, tungsten, tantalum and cobalt. However, various phase transformations that occur as function of temperature in PWA-1480 alloy are expected to be similar to Ni–Al–Cr system.

3.2 Atom Probe Field Ion Microscopy:

On cooling below the solidus temperature, on cooling γ' phase is expected to precipitate homogeneously within γ dendrites. It is speculated that, due to the nonequilibrium conditions, the partitioning between γ and γ' may lead to some interfacial segregation of elements such as tungsten and tantalum. This speculation can be investigated using the atom probe field ion microscopy technique. A field ion image of the PWA-1480 weld in the as-welded condition is shown in Fig. 5. The image shows the darkly imaged γ phase and the brightly imaged γ' precipitates. It is noteworthy that the interface between γ' and γ does not reveal any singularities characteristic of alloying element segregation. The atom probe composition profile obtained from this sample is shown in Fig. 6. As expected most of the aluminum, titanium, and tantalum partitioned to γ'. The elements cobalt, tungsten, and chromium partitioned to γ. As observed in FIM, no segregation was detected at γ–γ' interfaces contrary to the speculation. It is noteworthy that the alloying elements, including heavy elements such as tungsten and tantalum, are continuously partitioning between γ and γ' irrespective of rapid weld cooling conditions.

The APFIM measurements of γ and γ' compositions, in the PWA–1480 weld, are summarized in Table 2. The published APFIM compositions of γ and γ' phases [5–8] are also reported. The present results showed consistently that, except for one analysis, the aluminum concentrations of γ' were higher than 16 at.%. The average value is higher than the typical aluminum concentration of γ', 15-16 at.%, previously measured by APFIM [5-8]. The chromium concentration in the γ phase measured by Blavette et. al.[7], was 34 at.%. This value is higher than the 25 at.% measured in the present work. However, the other solute concentrations in γ' and γ were found to be similar with that measured by Miller et. al. [5]. The variations in γ and γ' compositions are attributed to the following reasons.

1. The thermodynamic calculations suggest that the composition of γ would be non uniform from the core to the boundary of the dendrite. Since the γ' particles precipitate from the γ phase during cooling, any variation in the composition of the γ phase will modify the γ' precipitation characteristics, such as the temperature at which precipitation occurs and the γ' phase composition.
2. The weld cooling conditions in electron beam welds can be greater than 100 K s^{-1}. At these rapid cooling conditions, the γ' precipitation characteristics will be complicated since equilibrium state is not achieved.

The reasons for the variation in the γ and γ' compositions may be a combination of both mechanisms mentioned above. Further work is necessary to characterize the segregation and nonequilibrium partitioning characteristics in these welds. It is also desirable to monitor the changes in the partitioning behavior in these welds on post–weld heat treatment and during thermal aging under service conditions.

3.3 Thermodynamic Calculation of γ–γ' Partitioning:

It is desirable to predict the partitioning behavior between γ and γ' with thermodynamic calculations using ThermoCalc™[9]. As a first confirmation of the predictive capability of ThermoCalc™, thermodynamic calculations are compared with published experimental results. Taylor and Floyd [13] studied various Ni-Al-Cr ternary compositions to measure the γ and γ' phase fields at various temperature. In their work series of Ni–Al–Cr alloys were homogenized and thermally aged at various temperatures. After thermal aging, the microstructures in the samples were characterized. The experimental compositional points studied by Taylor and Floyd [13] that lie in the γ and γ' phase fields at 1023 K are plotted with the calculated γ and γ' phase boundaries in the Ni-Al-Cr ternary system in Fig. 7. The figure shows excellent correlation between the experimental data points and the calculated phase boundaries. It could have been interesting to compare the APFIM data obtained from the PWA-1480 welds with the thermodynamic calculation in the Ni–Al–Cr–Ti–Ta–W–Co system. Unfortunately, due to the lack of data which describe the partitioning

characteristics of Ti, Ta, W, and Co between γ and γ' in the literature, exact partitioning calculations for the PWA–1480 welds can not be performed. However, for comparative purposes the measured APFIM data were normalized to nickel, aluminum and chromium concentrations and were compared with the calculations in the Ni-Al-Cr system at 1023 K. The comparisons are shown in Fig. 7. The calculations suggest that the solute partitioning experimentally measured in the PWA-1480 welds in the as-welded condition is slightly different from the calculated equilibrium partitioning. Further work is necessary to extend the thermodynamic calculations with consideration of other elements to predict the partitioning characteristics of γ and γ' during continuous cooling conditions and thermal aging conditions.

4. Summary

Branched dendritic structure was observed in a PWA–1480 single crystal superalloy electron beam weld fusion zone, in the as–welded condition. Blocky γ' phase was observed along the interdendritic regions. Fine cuboidal $L1_2$-ordered γ' precipitates (~ 75% volume fraction) were observed within γ dendrites. Atom probe analyses of elemental concentrations in γ and γ' phases showed small differences from previous APFIM analyses of commercial PWA–1480 single crystals. These differences may be due to the nonequilibrium nature of the phase transformations during the rapid weld cooling. No solute segregation was detected at the γ–γ' interfaces. APFIM results from PWA–1480 welds were also compared with the thermodynamic calculations.

Acknowledgment

This research was sponsored by the Division of Materials Sciences, U. S. Department of Energy, under contract DE-AC05-84OR21400 with Lockheed Martin Energy Systems, Inc. The authors thank Mr. R. P. Schaefer of United Technologies Pratt & Whitney for providing the PWA-1480 single crystal superalloy. The authors thank Mr. R. W. Reed and K. F. Russell for technical

assistance. The authors also thank Dr. G. M. Goodwin and Dr. P. J. Pareige of ORNL for reviewing the paper.

References

[1] M. L. Santella, Scripta Metall., 28 (1993) 1305.

[2] M. L. Santella and S. A. David, Welding Journal, 65 (1986) 129s.

[3] M. L. Santella, J. A. Horton, and S. A. David, Welding Journal, 67 (1988) 63s.

[4] S. A. David, W. A. Jemian, C. T. Liu, and J. A. Horton, Welding Journal, 64 (1985) 23s.

[5] M. K. Miller, R. Jayaram, L. S. Lin, and A. D. Cetel, Applied Surface Science, 76/77 (1994) 172.

[6] D. Blavette, A. Bostel and J. M. Sarrau, Metall. Trans., A., 16A (1985) 1703.

[7] D. Blavette, P. Caron and T. Khan, Scripta Metall., 20 (1986) 1395.

[8] D. Blavette, P. Caron and T. Khan, Proc. 6th Int. Symp. on Superalloys, Seven Springs, 1988, Eds. S. Reichman, D. N. Duhl, G. Maurer, S. Antolovich and C. Lund, The Metallurgical Society, Warrendale, PA, (1988) 305.

[9] B. Sundman, B. Jansson, and J. O. Andersson, Calphad 9 (1985) 153.

[10] M. K. Miller, J. Phys. 47 (1986) C7–493.

[11] Z. Scheil, Metallk, 34 (1942) 70.

[12] D. N. Duhl, in Superalloys II edited by C. T. Sims, N. S. Stoloff, and W. C. Hagel, John Wiley & Sons, New York, (1987) 189.

[13] A. Taylor and R. W. Floyd, Journal of the Institute of Metals, 81 (1952-53) 451.

DISCLAIMER

Tables

Table. 1 Composition of PWA 1480 cast single crystal superalloy.

Element	Wt.%	At.%
Al	5.0	11.0
Cr	10.0	11.5
Ti	1.5	1.9
Co	5.0	5.1
Ta	12.0	4.0
W	4.0	1.3
Ni	Balance	Balance

Table 2. Comparison of γ and γ' compositions measured by APFIM with the published results.

γ	Al	Cr	Ti	Co	Ta	W
1	4.6±0.5	27.2±1.0	0.5 ±0.2	8.8 ±0.6	0.5 ±0.1	2.8 ±0.4
2	4.4 ±0.5	25.7 ±1.1	0.5 ±0.2	9.6 ±0.7	0.6 ±0.2	3.7 ±0.4
3	4.6 ±0.4	23.5 ±0.9	0.4 ±0.1	9.8 ±0.6	1.4 ±0.2	2.4 ±0.3
4	4.6 ±0.7	25.4 ±1.4	0.4 ±0.2	9.4 ±0.9	0.8 ±0.3	2.9 ±0.5
Average†	4.6±0.5	25.5 ±1.0	0.4 ±0.2	9.4 ±0.7	0.8±0.2	2.9±0.4
Ref. 5	3.4±0.7	26.5±1.6	0.5±0.4	9.6±0.4	0.7±0.1	3.5±0.8
Ref. 7	2.79±0.1	34.03±0.4	0.17±0.1	11.0±0.2	0.56±0.1	2.15±0.1
γ'	Al	Cr	Ti	Co	Ta	W
1	20.0 ±0.9	2.6 ±0.3	2.3 ±0.3	3.1 ±0.4	6.1 ±0.5	1.9 ±0.3
2	18.4 ±0.9	2.1 ±0.3	2.4 ±0.4	2.6 ±0.4	6.7 ±0.6	1.1 ±0.2
3	18.7 ±1.2	2.8 ±0.5	2.5 ±0.5	2.4 ±0.5	6.9 ±0.8	1.6 ±.0.4
4	15.7 ±1.0	2.8 ±0.4	2.4 ±0.4	3.0 ±0.5	8.9 ±0.8	1.5 ±0.3
Average†	17.3 ±1.0	2.6 ±0.4	2.4 ±0.4	3.0 ±0.4	7.4 ± 0.7	1.3 ±0.3
Ref. 5	14.9±1.4	2.3±0.5	2.4±1.0	3.5±0.8	9.0±2.5	1.4±0.4
Ref. 7	15.4±0.2	2.17±0.1	2.85±0.1	3.1±0.1	4.59±0.1	1.68±0.1

† Average of four compositions.

Figure Captions

Fig. 1 Typical optical microstructure observed in a transverse section of the weld: (a) Low magnification micrograph showing the overall weld zone and (b) High magnification micrograph showing typical dendritic weld solidification.

Fig. 2. Transmission electron micrograph of the PWA-1480 weld metal region in the as-welded condition: (a) Low magnification picture showing two dendritic grains, dendritic boundary and blocky γ' phase (marked by an arrow) along the dendritic boundary. The electron diffraction pattern (inset of Fig. 2a), taken near to the $[001]_\gamma$ zone, shows the superlattice reflections from γ'; (b) High magnification picture showing the fine γ' distribution within the core of the γ dendrite.

Fig. 3. A quasi-binary diagram of the Ni-Al-Cr system with 11.5 at.% Cr calculated by ThermoCalc™ software [9]. The dotted line shows the composition corresponding to 11.0 at.% Al. In this phase diagram the tie lines are not in the plane of the diagram.

Fig. 4. Calculated variations of (a) liquid fractions and (b) composition of liquid and γ as a function of temperature during weld cooling for Ni-11.0 at.% Al - 11.5 at.% Cr alloy composition. The final liquid at ~1630 K may undergo a eutectic reaction as seen in Fig. 3.

Fig. 5 Field ion micrograph of γ matrix (dark region), γ' precipitates (bright) and the interfaces of γ–γ'. No evident interfacial segregation is observed.

Fig. 6 Atom probe concentration profile obtained from the PWA–1480 weld sample whose image in shown in Fig. 5. The interfaces and regions of γ and γ' are marked on the plot.

Fig. 7 Phase boundaries of γ and γ' at 1023 K calculated by ThermoCalc™[9] and experimental alloy compositions of Taylor and Floyd [13] in which only γ and γ' phases were present on aging at 1023 K. The plot also shows the comparison of APFIM partitioning characteristics between γ and γ' in PWA–1480 welds. The four compositions of γ and γ' given in Table 2, normalized to Ni, Al and Cr, are overlaid on the plot.

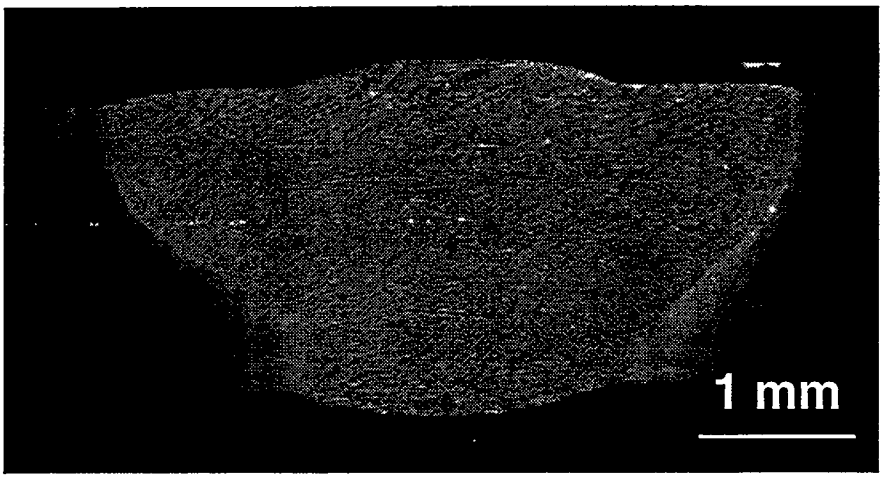

(a)

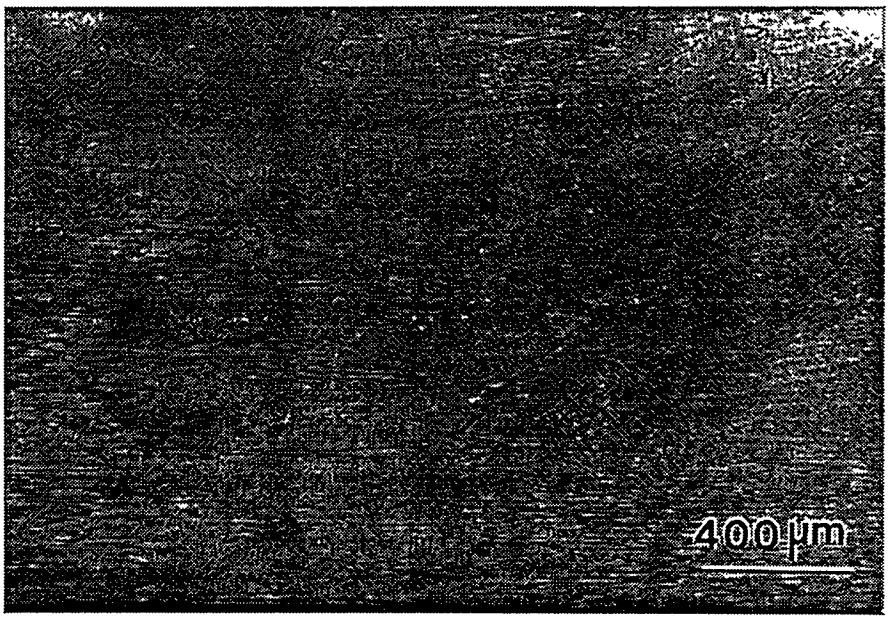

(b)

Fig. 1 Typical optical microstructure observed in a transverse section of the weld: (a) Low magnification micrograph showing the overall weld zone and (b) High magnification micrograph showing typical dendritic weld solidification..

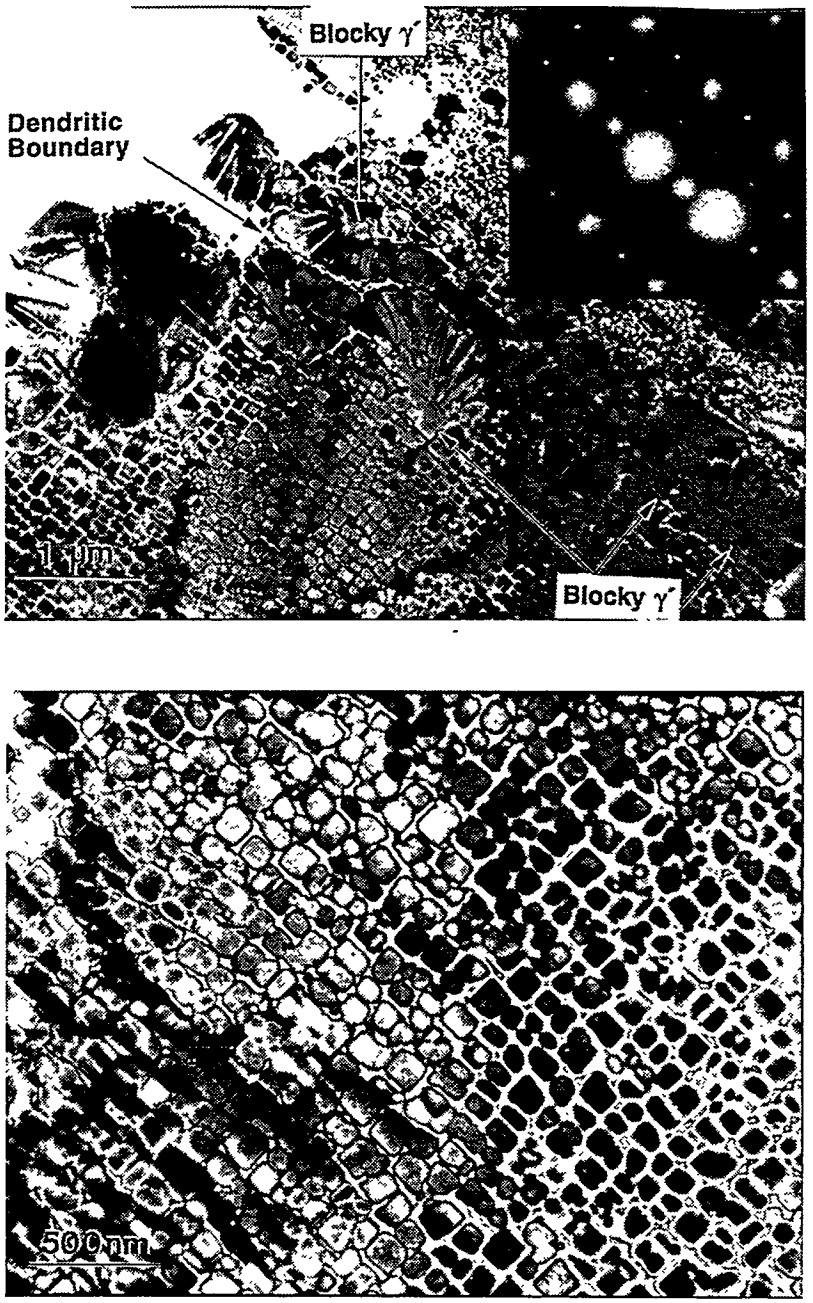

Fig. 2. Transmission electron micrograph of the PWA-1480 weld metal region in the as-welded condition: (a) Low magnification picture showing two dendritic grains, dendritic boundary and blocky γ' phase (marked by an arrow) along the dendritic boundary. The electron diffraction pattern (inset of Fig. 2a), taken near to the $[001]_\gamma$ zone, shows the superlattice reflections from γ'; (b) High magnification picture showing the fine γ' distribution within the core of the γ dendrite.

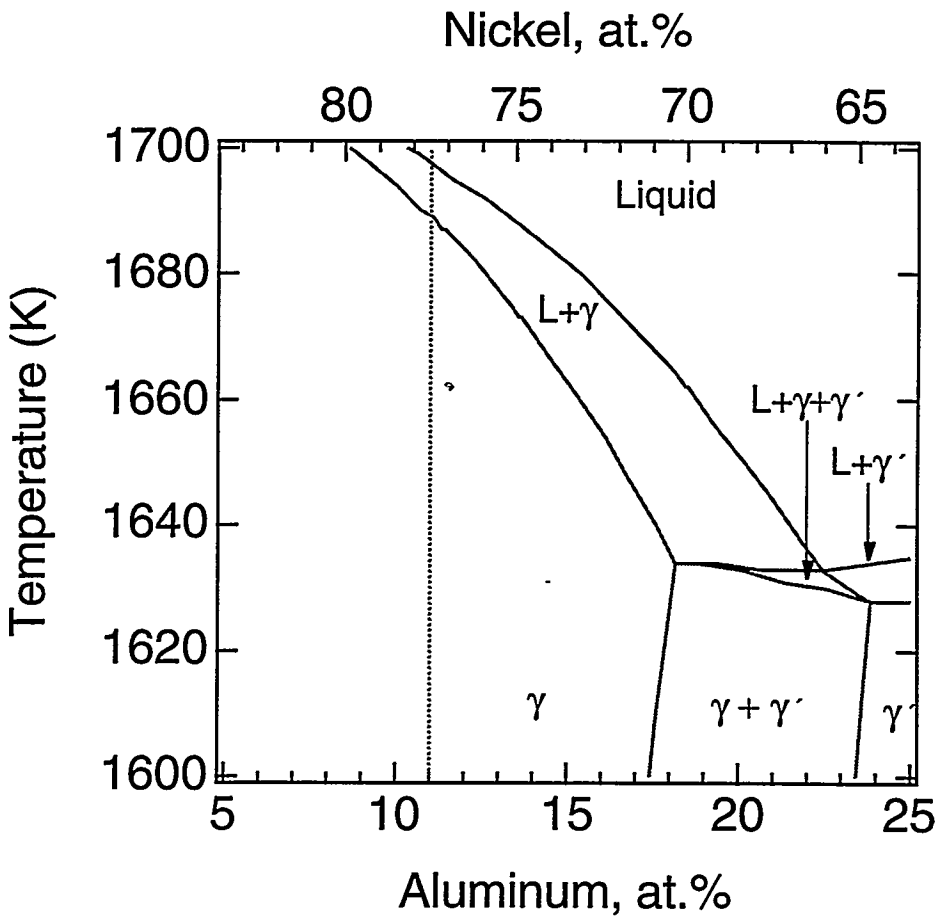
Nickel, at.%
80
75
70
65
1700
1680
1660
1640
1620
1600
Temperature (K)
Liquid
L+γ
L+γ+γ´
L+γ´
γ
γ + γ´
γ´
5
10
15
20
25
Aluminum, at.%

Fig. 3

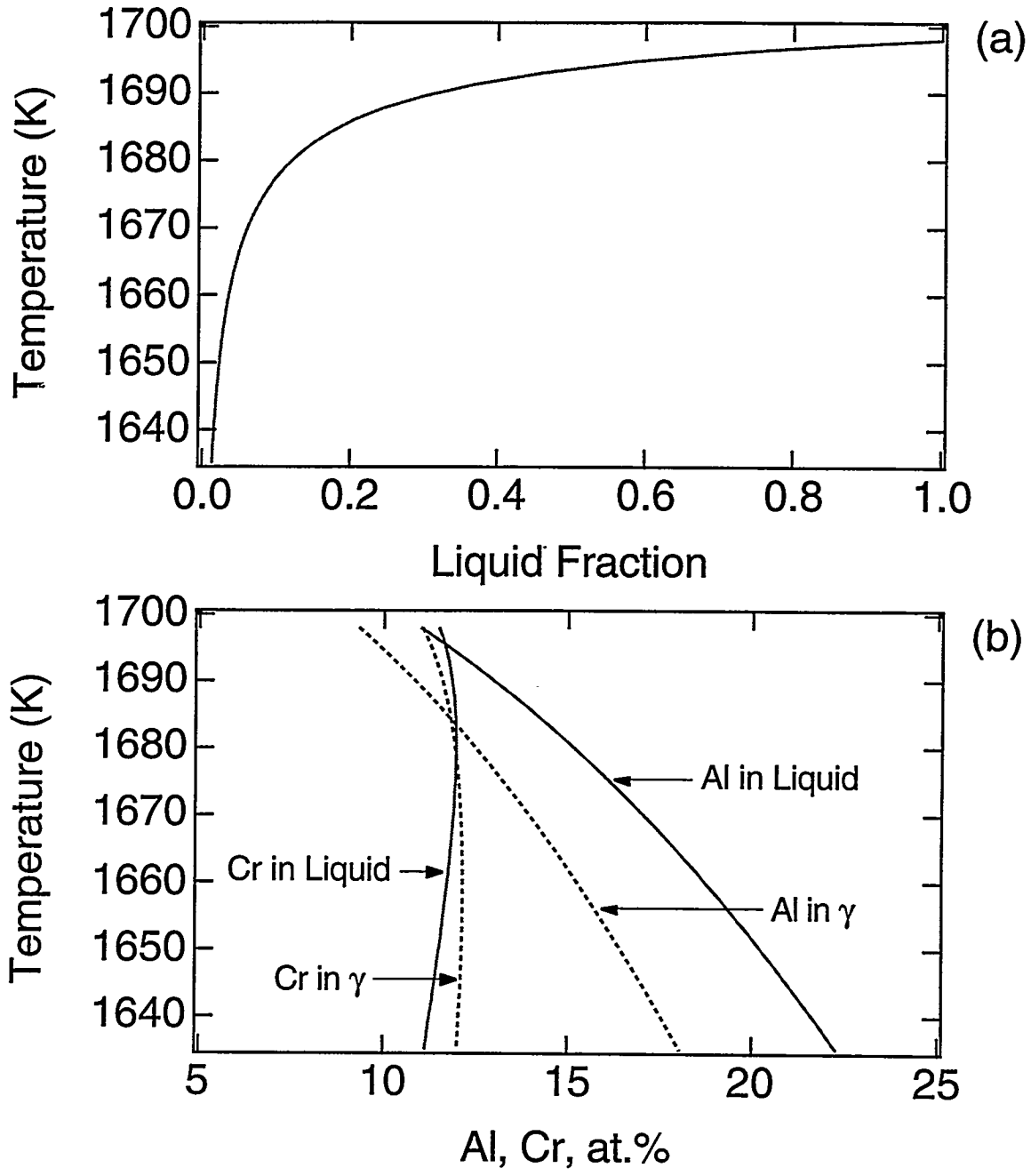
(a)
Temperature (K)
1700
1690
1680
1670
1660
1650
1640
0.0
0.2
0.4
0.6
0.8
1.0
Liquid Fraction
(b)
Temperature (K)
1700
1690
1680
1670
1660
1650
1640
Al in Liquid
Cr in Liquid
Al in γ
Cr in γ
5
10
15
20
25
Al, Cr, at.%

Fig. 4

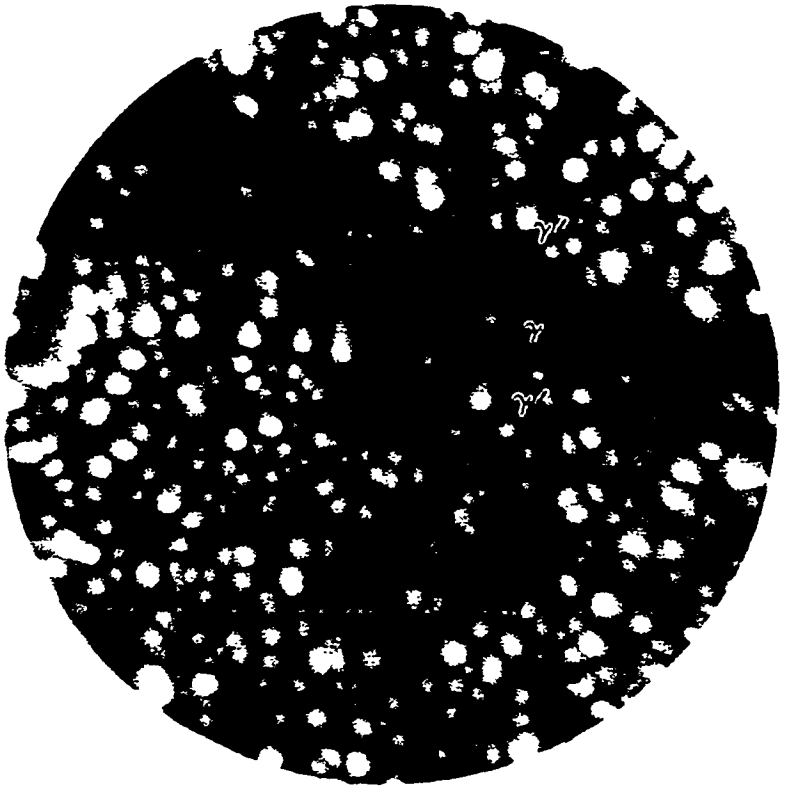

Fig. 5

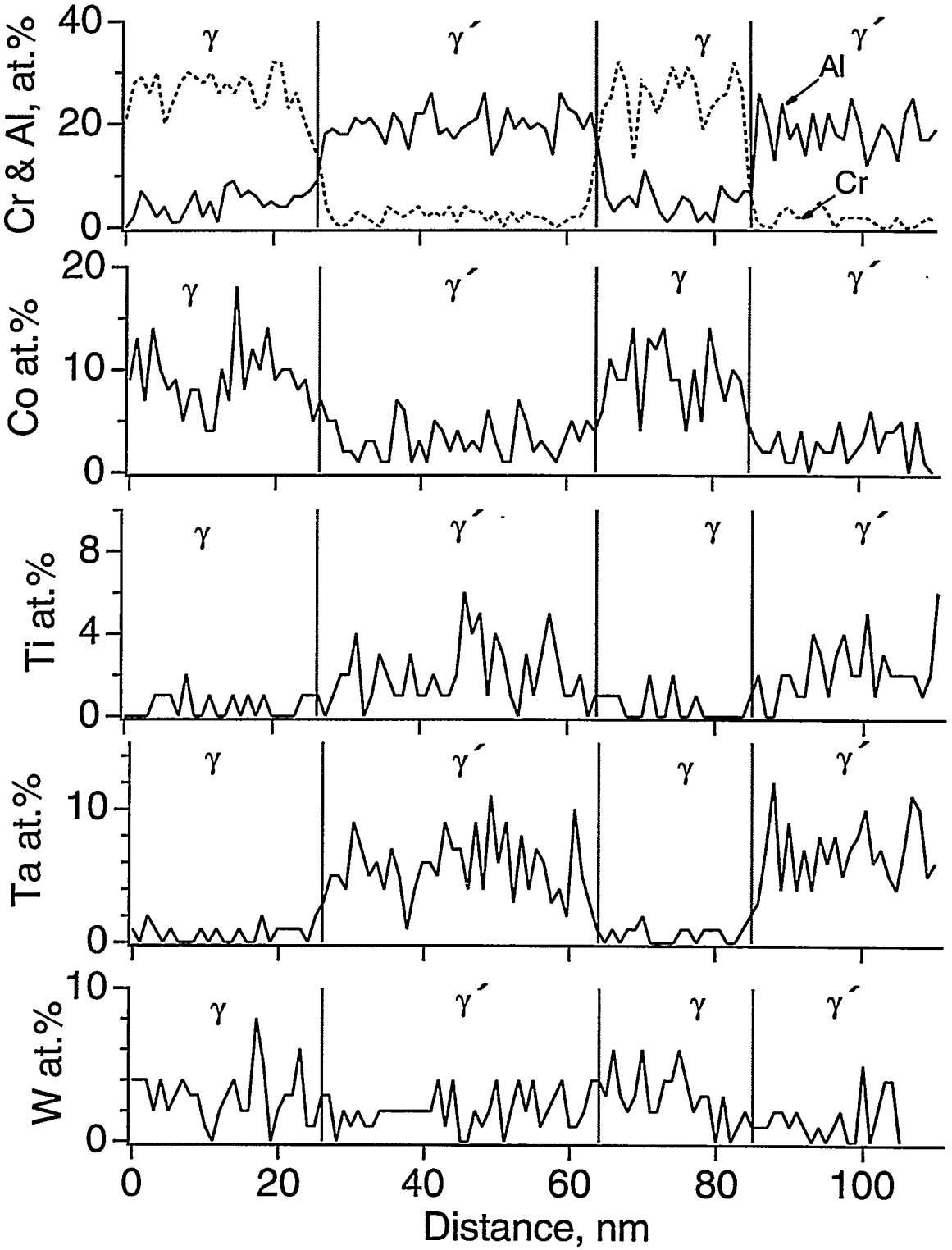
Cr & Al, at.%
40
20
0
γ
γ´
γ
γ´
Al
Cr
Co at.%
20
10
0
Ti at.%
8
4
0
Ta at.%
10
0
W at.%
10
0
0
20
40
60
80
100
Distance, nm

Fig.6